

Invariable mobility edge in a quasiperiodic lattice

Tong Liu(刘通), Shujie Cheng(成书杰), Rui Zhang(张锐), Rongrong Ruan(阮榕榕), and Houxun Jiang(姜厚勋)
Citation: Chin. Phys. B, 2022, 31 (**2**): 027101. DOI: 10.1088/1674-1056/ac140e
Journal homepage: http://cpb.iphy.ac.cn; http://iopscience.iop.org/cpb

What follows is a list of articles you may be interested in

Non-Hermitian Kitaev chain with complex periodic and quasiperiodic potentials

Xiang-Ping Jiang(蒋相平), Yi Qiao(乔艺), and Junpeng Cao(曹俊鹏)
Chin. Phys. B, 2021, 30 (**7**): 077101. DOI: 10.1088/1674-1056/abfa08

Surface potential-based analytical model for InGaZnO thin-film transistors with independent dual-gates

Yi-Ni He(何伊妮), Lian-Wen Deng(邓联文), Ting Qin(覃婷), Cong-Wei Liao(廖聪维), Heng Luo(罗衡), Sheng-Xiang Huang(黄生祥)
Chin. Phys. B, 2020, 29 (**4**): 047102. DOI: 10.1088/1674-1056/ab75d2

Dirac states from $p_{x,y}$ orbitals in the buckled honeycomb structures: A tight-binding model and first-principles combined study

Shi-Ru Song(宋士儒), Ji-Hui Yang(杨吉辉), Shi-Xuan Du(杜世萱), Hong-Jun Gao(高鸿钧), Boris I Yakobson
Chin. Phys. B, 2018, 27 (**8**): 087101. DOI: 10.1088/1674-1056/27/8/087101

Energy transfer between two aggregates in light-harvesting complexes

Wang Xiao-Lian, Li Hong-Rong, Zhang Pei, Li Fu-Li
Chin. Phys. B, 2013, 22 (**11**): 117102. DOI: 10.1088/1674-1056/22/11/117102

Invariable mobility edge in a quasiperiodic lattice

Tong Liu(刘通)[1,†], Shujie Cheng(成书杰)[2], Rui Zhang(张锐)[1], Rongrong Ruan(阮榕榕)[1], and Houxun Jiang(姜厚勋)[1]

[1] *School of Science, Nanjing University of Posts and Telecommunications, Nanjing* 210003, *China*
[2] *Department of Physics, Zhejiang Normal University, Jinhua* 321004, *China*

(Received 22 May 2021; revised manuscript received 23 June 2021; accepted manuscript online 14 July 2021)

We analytically and numerically study a 1D tight-binding model with tunable incommensurate potentials. We utilize the self-dual relation to obtain the critical energy, namely, the mobility edge. Interestingly, we analytically demonstrate that this critical energy is a constant independent of strength of potentials. Then we numerically verify the analytical results by analyzing the spatial distributions of wave functions, the inverse participation rate and the multifractal theory. All numerical results are in excellent agreement with the analytical results. Finally, we give a brief discussion on the possible experimental observation of the invariable mobility edge in the system of ultracold atoms in optical lattices.

Keywords: Anderson localization, quasiperiodic, mobility edge, multifractal

PACS: 61.44.Fw, 71.10.Fd, 71.23.An **DOI:** 10.1088/1674-1056/ac140e

1. Introduction

Anderson localization,[1] a universal phenomenon of wave propagation in disordered mediums, is an active research subject in condensed matter physics. With regard to the disordered systems, the scaling theory[2] predicts that delocalized-localized transitions are known to arise in dimension strictly higher than two. In one- and two-dimensional systems, uncorrelated random disturbances account for why all the wave functions are exponentially localized. Accordingly, in low-dimensional disordered systems, there is always a hot topic, namely the delocalization-localization transition. There is an energy level threshold which separates the delocalized functions from those are localized. This critical energy is known as the mobility edge. However, it is still a challenge to observe the mobility edge in three-dimensional (3D) systems with the mobility edge in experiment.[3–9] Therefore, to acquire more insights into the mobility edge and uncover its essence, low-dimensional systems, such as 1D quasiperiodic systems, are a better choice. After all, there has been a long history to search the systems with mobility edge and plenty of theoretical models are proposed and studied in decades.[10–23] Moreover, the mobility edge has been observed in recent experiments by manipulating the cold atoms trapped in 1D quasiperiodic optical lattice[24,25] although a precise measurement of its value is still lacking.

The Aubry–André (AA) model[26] plays an important role to understand the Anderson localization and uncover the mobility edge. As a paradigmatic 1D tight-binding model, the AA model has a self-dual symmetry, and the increasingly incommensurate potential will make the system undergo a localization transition, from the extended phase to the localized phase.[27] Moreover, the mobility edge always appears in the extended AA models. For instance, Das Sarma *et al.* revealed that there was mobility edge in a class of systems with slow-varying incommensurate on-site potentials.[10–12] Biddle *et al.* found the exactly solvable mobility edge in the extended AA model with long-range tunnelings.[13,14] Ganeshan *et al.* verified the existence of the mobility edge which was protected by the self-dual symmetry.[15] Liu *et al.* obtained the exactly solvable mobility edge in the off-diagonal incommensurate models.[16,17] Nowadays, the research about the mobility edge has been extended to the non-Hermitian case,[28–30] where the mobility edges were located in the real energy spectra. However, by comprehensively analyzing the above research results on mobility edge, we find that the mobility edges change with the extra parameters that are commonly the strength of the incommensurate on-site potentials. We cannot help but ask, is it a universal phenomenon that the mobility edge changes with the extra parameters? Is there a special case where the mobility edge is a constant that is a bit easier to measure experimentally?

In this work, we are motivated to study a 1D tight-binding model with tunable incommensurate potentials. We make attempt to find out whether there is a mobility edge which keeps a constant in this model and then extract it analytically, if it exists. We further verify the analytical result by the inverse participation rate and the spatial distributions of the wave functions.

The rest of this paper are arranged as follows: In Section 2 we present the model and derive the mobility edge by the self-dual relations. In Section 3 we verify the analytically obtained mobility edge by the inverse participation rate and the distributions of the wave functions. Finally, we make a summary in Section 4.

[†]Corresponding author. E-mail: t6tong@njupt.edu.cn

© 2022 Chinese Physical Society and IOP Publishing Ltd

2. Model and the mobility edge

In this section, we consider a 1D tight-binding model with nearest-neighbor hoppings and incommensurate on-site potentials, and we are devoted to extract the mobility edge analytically. The static Schrödinger equation is written as

$$E\psi_n = \psi_{n+1} + \psi_{n-1} + \frac{V}{1 - b\cos(2\pi\alpha n)}\psi_n, \tag{1}$$

where V is the potential strength with $0 < b < 1$ being the potential tuning parameter, α is irrational number, which makes the Hamiltonian incommensurate, and ψ_n is the amplitude of wave function at the nth lattice site. This model provides an extension of the quasi-periodic lattice previously introduced in Ref. [15] and displays a generalized self-duality. To derive the mobility edge, namely the critical energy E_c, which separates the extended wave functions from whose are localized, we first multiply both sides of Eq. (1) by $e^{i2\pi\alpha nm}$ and sum it over n. After setting $\phi_m = \sum_n e^{i2\pi\alpha nm}\psi_n$, we obtain

$$[E - 2\cos(2\pi\alpha m)]\phi_m = \sum_n e^{i2\pi\alpha nm}\frac{V}{1 - b\cos(2\pi\alpha n)}\psi_n. \tag{2}$$

Next, we introduce some self-dual relations, which are necessary in the following derivation:

$$\begin{aligned} &\cosh(s_0) = \frac{1}{b}, \quad E = 2\cosh(s), \\ &\Omega_m(s) = \frac{\cosh(s) - \cos(2\pi\alpha m)}{\sinh(s)}, \end{aligned} \tag{3}$$

where s and s_0 are real constants. Therefore, Eq. (2) can be rewritten as

$$2\sinh(s)\Omega_m(s)\phi_m = V\coth(s_0)\sum_{r'} e^{-|m-r'|s}\phi_{r'}. \tag{4}$$

Then, we multiply both sides of Eq. (4) by $\Omega_k(s_0)e^{i2\pi\alpha mk}$, and sum it over m. After defining the relationship $\varphi_k = \sum_m e^{i2\pi\alpha mk}\Omega_m(s)\phi_m$, Eq. (4) is further expressed as

$$2\sinh(s)\Omega_k(s_0)\varphi_k = V\coth(s_0)\sum_{k'} e^{-|k-k'|s}\varphi_{k'}. \tag{5}$$

We continue multiplying both sides of Eq. (5) by $e^{i2\pi\alpha kq}$, and summing it over k. By defining the relationship $\mu_q = \sum_k e^{i2\pi\alpha kq}\varphi_k$, Eq. (5) is transformed into

$$2\frac{\sinh(s)}{\sinh(s_0)}\cosh(s_0)\mu_q = \mu_{q-1} + \mu_{q+1} + V\frac{\coth(s_0)}{\Omega_q(s)}\mu_q. \tag{6}$$

Note that when $s = s_0$, Eq. (3) is reduced to Eq. (1). From the self-dual relations $\cosh(s) = 1/b$ and $E = 2\cosh(s)$, we obtain the mobility edge

$$E_c = 2/b. \tag{7}$$

Interestingly, for a fixed value of the tuning parameter b, E_c is independent of the potential strength V. The property of "being constant" of the mobility edge is a intriguing result. In the following, we will check the predictions of E_c in the theoretical analysis by direct numerical simulations, so as to make the theoretical analysis convictive.

3. Numerical results and discussions

In this section, we verify the accuracy of the analytically obtained mobility edge E_c by exhaustively numerical analysis. In order to acquire the eigenenergies E of the system and the associated wave functions ψ, we numerically diagonalize the model's Hamiltonian which is defined in terms of the Schrödinger equation in Eq. (1). Then, it is convenient to calculate other typically physical quantities that are needed in our numerical validation. For example, the inverse participation rate and the spatial distributions of the wave functions will be used to distinguish the extended and localized states. Although our numerical simulations are carried out at the system with finite size, our results are exactly consistent with the theoretical analysis under the thermodynamic limit.

To begin with, we calculate the inverse participation rate (IPR). As it was studied in Ref. [31], the IPR of a given wave function ψ is defined as

$$\mathrm{IPR}_j = \sum_{n=1}^{L} |\psi_n^j|^4, \tag{8}$$

where ψ has been normalized, L is the total number of the lattice sites, and j denotes the energy level index. It is widely known that for the extended wave functions, the corresponding IPRs scale like L^{-1}, which tend to 0 when $L \to \infty$, whereas they keep finite values for localized states.

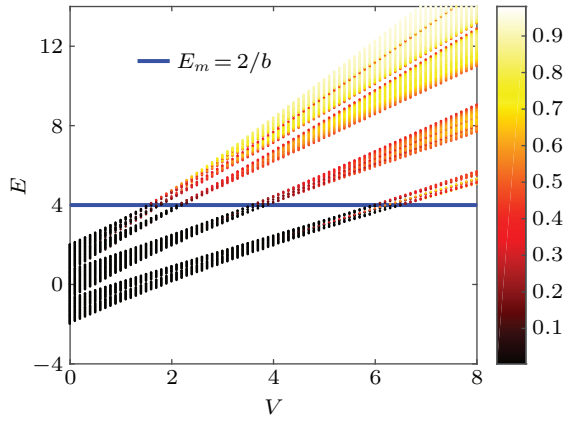


Fig. 1. The eigenvalues of Eq. (1) and IPR as a function of V with the parameter $b = 0.5$. The total number of sites is set to be $L = 500$. Different colors of the eigenvalue curves indicate different magnitudes of the IPR of the corresponding wave functions. The black region where the IPR approaches zero denotes the extended states, and the orange region with a whitish hue where the IPR tends to 1 denotes the localized states. The blue solid line represent the boundary between spatially localized and extended states, i.e., the mobility edge $E_c = 2/b = 4$.

Figure 1 is the energy spectrum which exhibits variation of eigenenergies E as a function of the parameter V, where we have considered the size of the system is $L = 500$ and the tuning parameter $b = 0.5$. As shown in Fig. 1, the spectrum is not a single band but consists of several bands. The color shows the IPR of the corresponding eigenenergy. Concretely, the black region where the IPR approaches zero means the wave functions that these eigrnenergies correspond to are all extended. On the contrary, the orange region with a whitish hue where the IPR tends to 1 means the wave functions that these eigen-energies correspond to are all localized. Intuitively, there is a critical energy $E_c = 4$ separating the extended states and the localized states. The result of this numerical analysis is consistent with what the theoretical analysis predicts.

In order to have an intuitive insight into the separation in the aspect of energy, we plot the spatial distributions of associated wave functions, whose corresponding eigenenergies are near E_c. Before performing the numerical calculation, we have specified that the required parameters are $b = 0.5$, $V = 3.8$ and $L = 5000$. We choose three typical wave functions whose corresponding eigenenergies are above, below or close to the mobility edge $E_c = 4$. Figure 2 shows the spatial distributions of the four wave functions, in which Fig. 2(a) is intuitively seen that the wave function is extended, whose corresponding energy is below $E_c = 4$. On the contrary, Fig. 2(c) is the localized states, whose corresponding energy is above $E_c = 4$. More impressive, the eigenenergy of Fig. 2(b) is closed to $E_c = 4$ and can be seen as be neither localized nor extended over the whole space, instead, it displays the characteristic of the critical state.

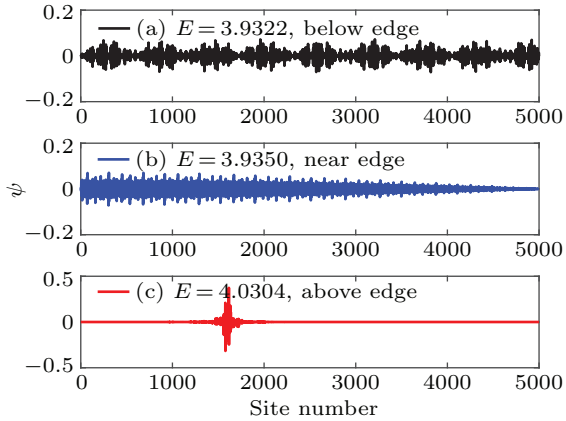


Fig. 2. Wave functions obtained from Eq. (1) with $b = 0.5$, $V = 3.8$ and $L = 5000$ nearby the mobility edge $E_c = 4$. Three different eigenenergies: (a) low energy extended state below the mobility edge, (b) critical state near the mobility edge, and (c) high energy localized state above the mobility edge.

To further verify the reliability of the analysis results of IPR and wave functions, we use the multifractal theory, which has been widely applied to standard quasiperiodic models.[32] For each wave function ψ_n^j, a scaling exponent β_n^j can be extracted from the nth on-site probability $P_n^j = |\psi_n^j|^2 \sim (1/F_m)^{\beta_n^j}$. According to the multifractal theorem, when the wave functions are extended, the maximum of P_n^j scales as $\max(P_n^j) \sim (1/F_m)^1$, i.e., $\beta_{\min}^j = \min(\beta_n^j) = 1$. On the other hand, when the wave functions are localized, P_n^j peaks at very few sites and nearly zero at the other sites, yielding $\max(P_n^j) \sim (1/F_m)^0$ and $\beta_{\min}^j = \min(\beta_n^j) = 0$. As for the critical wave functions, the corresponding $\beta_{\min}^j$ is located within the interval $(0, 1)$, and can be used to discriminate extended and critical states. In order to reduce finite-size effects, we use $\beta_{\min}^j$ to distinguish different wave functions in numerical calculations.

Figure 3 plots $\beta_{\min}$ as a function of the inverse Fibonacci index $1/m$. It clearly shows that $\beta_{\min}$ is between 0 and 1 in the large L limit for the eigenenergy $E = 4.0$, hence suggesting that wave functions closed to the mobility edge are critical. However, for the eigenenergy $E = 3.9$, $\beta_{\min}$ asymptotically tends to 1 in the thermodynamic limit, indicating that the corresponding wave function is extended. Conversely, for the eigenenergy $E = 4.1$, $\beta_{\min}$ asymptotically tends to 0 in the thermodynamic limit, indicating that the corresponding wave function is localized. Thus, the above numerical results are in excellent agreement with the analytical results. We have also checked other combinations of parameters and get the same results as expected.

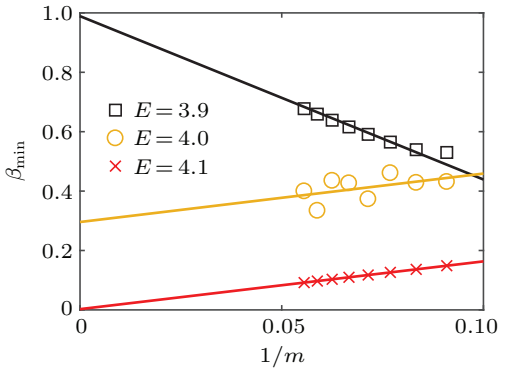


Fig. 3. Behavior of $\beta_{\min}$ as a function of the inverse Fibonacci index $1/m$ for various eigenenergies when $V = 3.75$. The brown markers correspond to the critical state with $E = 4.0$ closed to the mobility edge E_c, the black markers correspond to the extended state with $E = 3.9$ below the mobility edge E_c, and the red markers correspond to the localized state with $E = 4.1$ above the mobility edge E_c.

Finally, we would like to point out that this invariable mobility edge can be realized in the ultracold-atom experiment. Using synthetic lattices of laser-coupled atomic momentum modes, the authors of Ref. [33] experimentally realized a recently proposed family of nearest-neighbor tight-binding models having quasiperiodic site energy modulation that host an variable mobility edge protected by a duality symmetry. The experimental method in this paper is based on momentum space lattice tuning. The on-site potential at each lattice point in momentum space is equal to the detuning of Raman coupling between different momentum states, hence the on-site potential form required for the precise modulation of these detuning to match is obtained.

Alternatively, we can utilize synthetic dimension to simulate this type of on-site lattice. For example, we can use each spin state of large spin atoms (such as Dy atoms) as lattice points, and use Raman Coupling to couple adjacent spins (i.e., the coupling of adjacent lattice points), then realize the on-site potential by controlling the detuning property of Raman coupling.[34–36]

4. Summary

In conclusion, we have studied a 1D tight-binding model with tunable quasi-periodic potential. It is revealed that there exists mobility edge in this model, and its analytical expression is obtained by the self-dual relations. Surprisingly, unlike previous studies, the mobility edge in our model keeps invariable with the strength of the potential, which is only determined by the control parameter b. This finding may contribute to a more convenient observation of the mobility edge in the future experiment. Detailed numerical analyses, such as the inverse participation rate and the spatial distributions of wave functions, demonstrate that our results are reliable.

Acknowledgements

T. Liu acknowledges X.-J. Liu for fruitful discussion. This work was supported by the Natural Science Foundation of Jiangsu Province, China (Grant No. BK20200737), NUPTSF (Grants Nos. NY220090 and NY220208), and the National Natural Science Foundation of China (Grant No. 12074064), and the Innovation Research Project of Jiangsu Province, China (Grant No. JSSCBS20210521), and NJUPT-STITP (Grant No. XYB2021294).

References

[1] Anderson P W 1958 *Phys. Rev.* **109** 1492
[2] Abrahams E, Anderson P W, Licciardello D C and Ramakrishnan TV 1979 *Phys. Rev. Lett.* **42** 673
[3] Semeghini G, Landini M, Castilho P, Roy S, Spagnolli G, Trenkwalder A, Fattori M, Inguscio M and Modugno G 2015 *Nat. Phys.* **11** 554
[4] Skipetrov S E, Minguzzi A, van Tiggelen B A and Shapiro B 2008 *Phys. Rev. Lett.* **100** 165301
[5] Piraud M, Pezzé L and Sanchez-Palencia L 2012 *Europhys. Lett.* **99** 50003
[6] Piraud M, Pezzé L and Sanchez Palencia L 2013 *Phys.* **15** 075007
[7] Delande D and Orso G 2014 *Phys. Rev. Lett.* **113** 060601
[8] Jendrzejewski F, Bernard A, Müller K, Cheinet P, Josse V, Piraud M, Pezzé L, Sanchez Palencia L, Aspect A and Bouyer P 2012 *Nat. Phys.* **8** 398
[9] Sanchez Palencia L 2015 *Nat. Phys.* **11** 525
[10] Das Sarma S, He S and Xie X C 1988 *Phys. Rev. Lett.* **61** 2144
[11] Das Sarma S, He S and Xie X C 1990 *Phys. Rev. B* **41** 5544
[12] Liu T, Yan H Y and Guo H 2017 *Phys. Rev. B* **96** 174207
[13] Biddle J and Das Sarma S 2010 *Phys. Rev. Lett.* **104** 070601
[14] Biddle J, Priour D J, Wang B and Das Sarma S 2011 *Phys. Rev. B* **83** 075105
[15] Ganeshan S, Pixley J H and Das Sarma S 2015 *Phys. Rev. Lett.* **114** 146601
[16] Liu T, Xianlong G, Chen S and Guo H 2017 *Phys. Lett. A* **381** 3683
[17] Liu T and Guo H 2018 *Phys. Rev. B* **98** 104201
[18] Yin H, Hu J, Ji A C, Juzeliunas G, Liu X J and Sun Q 2020 *Phys. Rev. Lett.* **124** 113601
[19] Wang Y, Zhang L, Niu S, Yu D and Liu X J 2020 *Phys. Rev. Lett.* **125** 073204
[20] Wang Y, Xia X, Zhang L, Yao H, Chen S, You J, Zhou Q and Liu X J 2020 *Phys. Rev. Lett.* **125** 196604
[21] Yao H, Khouldi H, Bresque L and Sanchez-Palencia L 2019 *Phys. Rev. Lett.* **123** 070405
[22] Yao H, Giamarchi T and Sanchez-Palencia L 2020 *Phys. Rev. Lett.* **125** 060401
[23] Liu T, Xia X, Longhi S and Sanchez-Palencia L 2021 arXiv:2105.04591
[24] Lüschen H P, Scherg S, Kohlert T, Schreiber M, Bordia P, Li X, Das Sarma S and Bloch I 2018 *Phys. Rev. Lett.* **120** 160404
[25] An F A, Meier E J and Gadway B 2018 *Phys. Rev. X* **8** 031045
[26] Aubry S and André G 1980 *Ann. Isr. Phys. Soc.* **3** 18
[27] Goblot V, Strkalj A, Pernet N, Lado J L, Dorow C, Lemaître A, Le Gratiet L, Harouri A, Sagnes I, Ravets S, Amo A, Bloch J and Zilberberg O 2020 *Nat. Phys.* **16** 832
[28] Liu Y, Jiang X P, Cao J and Chen S 2020 *Phy. Rev. B* **101** 174205
[29] Liu T, Guo H, Pu Y and Longhi S 2020 *Phys. Rev. B* **102** 024205
[30] Zeng Q B, Yang Y B and Xu Y 2020 *Phys. Rev. B* **101** 020201
[31] Thouless D J 1974 *Phys. Rep.* **13** 93
[32] Kohmoto M and Tobe D 2008 *Phys. Rev. B* **77** 134204
[33] Alex An F, Padavić K, Meier E J, Hegde S, Ganeshan S, Pixley J H, Vishveshwara S and Gadway B 2021 *Phys. Rev. Lett.* **126** 040603
[34] Song B, He C, Niu S, Zhang L, Ren Z, Liu X J and Jo G B 2019 *Nat. Phys.* **15** 911
[35] Yi C R, Zhang L, Zhang L, Jiao R H, Cheng X C, Wang Z Y, Xu X T, Sun W, Liu X J, Chen S and Pan J W 2019 *Phys. Rev. Lett.* **123** 190603
[36] Ji W, Zhang L, Wang M, Zhang L, Guo Y, Chai Z, Rong X, Shi F, Liu X J, Wang Y and Du J 2020 *Phys. Rev. Lett.* **125** 020504